Generation of Coherent Sub-Terahertz Carrier with Phase Stabilization for Wireless Communications

Yasuyuki Yoshimizu, Shintaro Hisatake, Shigeru Kuwano, Jun Terada, Naoto Yoshimoto, and Tadao Nagatsuma

Abstract: **In this paper, we present a photonic approach for generating highly stable coherent sub-terahertz (THz) signals for wireless communications. As proof-of-concept we transmit data at 100 GHz carrier frequency using on-off keying modulation and heterodyne detection. The sub-THz carrier signals are generated by photo-mixing two optical carrier signals at different frequencies, extracted from an optical frequency comb. We introduce a novel system to stabilize the phase of the optical carrier signals. Error-free transmission is successfully achieved up to a bit rate of 8.5 Gbit/s at 100 GHz.**

Index Terms: **Coherent carrier, optical frequency comb, phase stabilization, THz wave.**

I. INTRODUCTION

Terahertz (THz) wireless communication has attracted a great deal of interest for the short-distance transmission of ultrahigh data-rate signals such as high-definition television (HDTV) and 4K-TV signals [1], [2]. Until now, 30 Gbit/s error-free (bit error rate (BER)$< 10^{-11}$) transmission has been demonstrated using intensity modulation and direct detection scheme at 300 GHz [3], [4]. One of the promising ways to enhance the data rate is to introduce multi-level modulation techniques such as quadrature phase-shift keying (QPSK) and quadrature amplitude modulation (QAM) using coherent THz carrier signals [5]–[13]. Photonic generation and modulation of a THz carrier in a coherent wireless link will be a key technology. There are several techniques for the photonics-based THz carrier generation using a pair of free-running lasers [5]–[10], an optical frequency comb (OFC) [11]–[13], and a mode-locked-pulse laser [14]. The use of monochromatic continuous-wave THz carriers is suitable for the future optical/wireless seamless networks where data signals are delivered through optical fiber cables and air without any change in the modulation format.

As an example of the free-running laser-based approach, photonically up-converted 25 Gbit/s fiber-wireless QPSK data transmission ($\mathrm{BER} > 10^{-6}$) link at the W-band (75–110 GHz) has been demonstrated [5]. The carrier was generated by photo-mixing two frequency-detuned (87.5 GHz) free-running lasers. In this incoherent radio-over-fiber (RoF) system, a digital-signal-processing (DSP)-based receiver was employed for offline digital down-conversion and signal demodulation, together with carrier phase noise correction.

The OFC-based carrier generation has been demonstrated in 40 Gbit/s ($\mathrm{BER} = 1.90\times10^{-3}$) W-band 16-QAM RoF system [12]. In this system, the frequency-detuned optical signals for THz carrier generation were extracted from the OFC with an optical arrayed-waveguide grating (AWG) filter and were coupled with a fiber coupler. Each OFC component is phase-locked before the extraction using the AWG filter. However, the pass length of the optical fiber between the AWG filter and the fiber coupler fluctuates due to temperature fluctuation and acoustic noise. Therefore, the phases of the two modes fluctuate independently, and the generated carrier shows phase fluctuations. This system also requires DSP-based carrier phase noise correction at the receiver side. One of the effective ways to reduce the phase fluctuation is to integrate the AWG filter and the optical coupler on a planar light-wave circuit (PLC) substrate in order to keep the optical path length difference between the two modes constant [13]. At this point, however, it is a challenging issue to integrate active devices like optical modulators on PLC to realize such OFC-based systems as proposed in [12].

In this paper, we propose a practical phase stabilization scheme in the OFC-based sub-THz carrier generation without the use of PLCs in the transmitter, and demonstrate error-free data transmission without the use of DSP and error correction in the receiver. In Section II, we explain our approach to stabilizing the OFC-based carrier signal generation and show how the phase changes in the system without stabilization described in previous study. Next, we describe our experimental system based on on-off keying modulation and heterodyne detection schemes in Section III. In Section IV, we show an 8.5 Gbit/s ($\mathrm{BER} < 10^{-11}$) data transmission at 100 GHz carrier frequency as a proof-of-concept experiment.

II. PHASE STABILIZATION SYSTEM

Fig. 1 shows the conceptual diagram of the sub-THz wave generation system with an OFC generator. The phase of a single frequency laser is modulated with two electro-optic modulators (EOMs) to generate the OFC. The carrier signals are generated by photo-mixing two optical carrier signals at different frequencies, extracted from the OFC using an AWG filter. The phases of the optical carriers ($\phi_1(t)$ and $\phi_5(t)$) in the optical fiber cables between the AWG filter and the optical fiber coupler (OC) fluctuate independently due to temperature fluctuations and acoustic noise. The coherence of the sub-THz wave is dependent on the

Manuscript received July 1, 2013.

Y. Yoshimizu, S. Hisatake, and T. Nagatsuma are with Graduate School of Engineering Science, Osaka University, 1-3 Machikaneyama, Toyonaka, Osaka 560-8531, Japan, email: yasuyukiyoshimizu093@s.ee.es.osaka-u.ac.jp, {hisatake, nagatuma}@ee.es.osaka-u.ac.jp.

S. Kuwano, J. Terada, and N. Yoshimoto are with NTT Access Network Service Systems Laboratories, NTT Corporation, 1-1Hikarino-oka, Yokosuka, Kanagawa 239-0847, Japan, email: {kuwano.shigeru, terada.jun, yoshimoto.naoto}@lab.ntt.co.jp.

Digital object identifier 10.1109/JCN.2013.000105

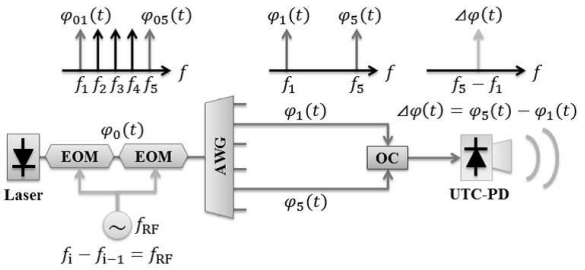

Fig. 1. The conceptual diagram of the sub-THz wave generation.

stability of the phase differences of the optical carriers, as shown in the equation below:

$$\Delta\phi(t) = \phi_5(t) - \phi_1(t). \tag{1}$$

Therefore, phase fluctuations in the optical fiber cables between the AWG filter and the OC are a practical problem in the OFC-based coherent sub-THz carrier generation. In our scheme, $\Delta\phi(t)$ is stabilized by locking the phases of the two optical carriers ($\phi_1(t)$ and $\phi_5(t)$) to those of the OFC signals ($\phi_{01}(t)$ and $\phi_{05}(t)$), where the relative phases between the OFC components are mutually locked.

Fig. 2 shows a schematic diagram of the stabilization system with a proportional-integral-derivative (PID) controller.

In our stabilization system, a dither signal is applied to the phase of the optical carrier with a phase shifter (PS) to detect the phase fluctuation ($\phi_1(t) - \phi_{01}(t)$) relative to the phase of the reference OFC, where $\phi_{01}(t)$ is the phase of f_1 component of the OFC. We express the optical carrier ($F_1(t)$) and the dither signal ($F_{\mathrm{d1}}(t)$) as in the equations below:

$$F_1(t) = \cos[\omega_1 t + \phi_1(t)], \tag{2}$$

$$F_{\mathrm{d1}}(t) = V_m \sin\omega_{\mathrm{d1}} t \tag{3}$$

where $\omega_1 = 2\pi f_1$, $\omega_{\mathrm{d1}} = 2\pi f_{\mathrm{d1}}$ and f_1 and f_{d1} are the frequencies of the optical carrier and the dither signal, respectively, and V_m is the amplitude of the dither signal. Thus, the carrier which is modulated by the dither signal is expressed as

$$F_1(t) = \cos[\omega_1 t + \phi_1(t) + m\sin\omega_{\mathrm{d1}} t], \tag{4}$$

$$m = \frac{\pi V_m}{2V_\pi} \tag{5}$$

where m is the modulation index and V_π is the half-wave voltage of the PS.

The modulated carrier and the reference OFC are coupled at the OC, and detected by using a slow PD with a cutoff frequency f_{c} of 33 kHz. Because the PD cutoff frequency is much lower than the OFC spacing ($f_{\mathrm{c}} << f_{\mathrm{RF}}$), the photo-mixing signal between optical carriers of the same frequency is output. That is, the phase fluctuation relative to the phase of the OFC is down-converted. At point (A) in the Fig. 2, the normalized AC component of the output signal I_1 can be expressed as

$$\begin{aligned} I_1 &= \cos[\phi_1(t) - \phi_{01}(t) + m\sin\omega_{\mathrm{d1}} t] \\ &= \sum_{-\infty}^{\infty} \{J_n(m)\cos[\phi_1(t) - \phi_{01}(t) + n\omega_{\mathrm{d1}} t]\} \end{aligned} \tag{6}$$

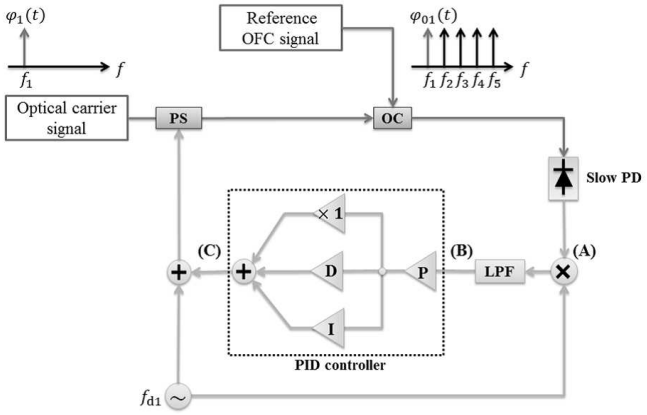

Fig. 2. Schematic diagram of the stabilization system with the PID controller.

where J_{n} is a Bessel function of the first kind.

By mixing the PD output signal with the dither signal and cutting off the higher frequency component with a low pass filter (LPF), at point (B), the phase fluctuation is detected as a voltage error signal.

$$V_1 \propto \sin[\phi_1(t) - \phi_{01}(t)]. \tag{7}$$

When $\phi_1(t) - \phi_{01}(t)$ is small,

$$V_1 \propto \phi_1(t) - \phi_{01}(t). \tag{8}$$

The detected error signal is negatively fed back to the PS through a PID controller to stabilize the relative phase of $\phi_1(t) - \phi_{01}(t)$. To minimize the phase fluctuation, the proportional term provides a proportional control action to the phase fluctuation, the integral term reduces the steady-state phase fluctuation (phase offset), and the derivative term improves the transient response [15]. At point (C), the output signal of the PID controller V_{PID} is given as

$$V_{\mathrm{PID}} = G_{\mathrm{P}} \times \left[V_1 + G_{\mathrm{I}} \int V_1 dt + G_{\mathrm{D}} \frac{d}{dt} V_1 \right] \tag{9}$$

where G_{P} is the proportional gain, G_{I} is the integral gain, and G_{D} is the derivative gain. When the error signal is zero, the phase of the optical carrier is locked to that of the OFC:

$$\phi_1(t) - \phi_{01}(t) = 0. \tag{10}$$

Fig. 3 shows a schematic diagram of the coherent sub-THz wave generator with the phase stabilization system. To generate a coherent sub-THz wave, the phases of the two OFC components should be stabilized simultaneously. Therefore, the dither signals with frequencies of f_{d1} and f_{d5} are applied to the optical carriers whose frequencies are f_1 and f_5, respectively. The output signal from the slow PD consists of three components: V_{DC}, I_1, and I_5. The normalized AC components are:

$$\begin{aligned} I_1 &= \cos[\phi_1(t) - \phi_{01}(t) + m\sin\omega_{\mathrm{d1}} t] \\ &= \sum_{-\infty}^{\infty} \{J_n(m)\cos[\phi_1(t) - \phi_{01}(t) + n\omega_{\mathrm{d1}} t]\}, \end{aligned} \tag{11}$$

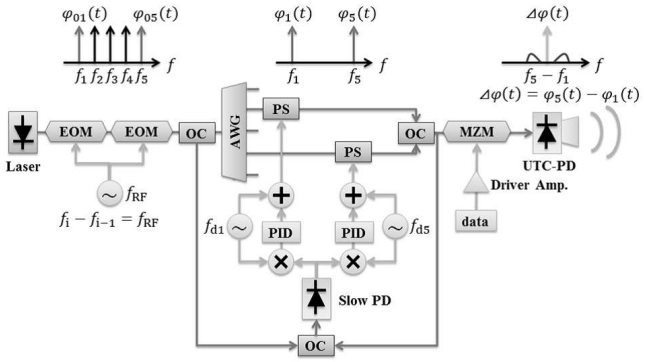

Fig. 3. Schematic diagram of the coherent sub-THz wave generator with a phase stabilization system.

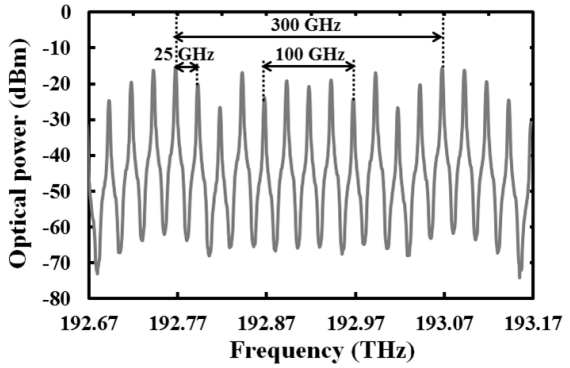

Fig. 4. Measured OFC spectra (resolution bandwidth: 0.02 nm).

$$I_5 = \cos[\phi_5(t) - \phi_{05}(t) + m\sin\omega_{d5}t] = \sum_{-\infty}^{\infty}\{J_n(m)\cos[\phi_5(t) - \phi_{05}(t) + n\omega_{d5}t]\} \quad (12)$$

where $\omega_{d5} = 2\pi f_{d5}$ and f_{d5} is the frequency of the dither signal for the f_5 component.

By mixing the PD output signal with two dither signals independently, phase fluctuations relative to the phase of the OFC are detected as follows

$$V_1 \propto \sin[\phi_1(t) - \phi_{01}(t)], \quad (13)$$

$$V_5 \propto \sin[\phi_5(t) - \phi_{05}(t)]. \quad (14)$$

In our stabilization system, each phase fluctuation relative to the phases of the OFC can be detected separately, even when there are multiple optical carriers. Therefore, our technique can be extended to multi-carrier format, such as orthogonal frequency-division multiplexing (OFDM).

The detected phase fluctuations are negatively fed back to PSs through PID controllers, to stabilize the sub-THz phase fluctuation. Under phase stabilization, the phase of the generated sub-THz wave can be expressed as

$$\Delta\phi(t) = \phi_5(t) - \phi_1(t) = \phi_{05} - \phi_{01} \quad (15)$$

where $\phi_{05} - \phi_{01}$ is a constant value, due to the OFC.

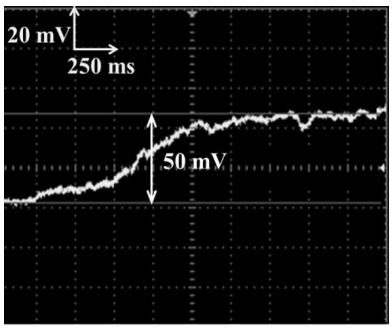

Fig. 5. Typical fluctuation of V_1. 50 mV corresponds to π.

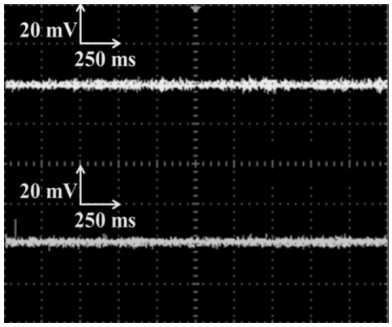

Fig. 6. Detected fluctuations with phase stabilization. Upper trace: V_1. Lower trace: V_5.

III. WIRELESS LINK USING COHERENT SUB-THZ CARRIER

In the experiment, a single frequency laser was modulated at $f_{RF} = 25$ GHz with the two EOMs to generate an OFC signal in the transmitter shown in Fig. 3. Fig. 4 shows the OFC spectra measured at the resolution bandwidth of 0.02 nm. We confirmed that our transmitter is capable of generating a carrier frequency of more than 300 GHz as shown in Fig. 4. As a proof-of-concept, we will generate a 100 GHz coherent carrier signal and apply it to a wireless link.

In the stabilization system, $f_{d1} = 12.8$ kHz and $f_{d5} = 16$ kHz. The cutoff frequency of the slow PD was $f_c = 33$ kHz. The parameters of the PID controller were $G_P = 1.0 \times 10$, $G_I = 1.0 \times 10^3$ s, and $G_D = 1.0 \times 10^{-5}$ 1/s. A piezoelectric transducer (PZT) was used as the PS. The bandwidth of the closed loop was about 20 Hz.

Fig. 5 shows the typical phase fluctuations of $\phi_1(t) - \phi_{01}(t)$ detected as voltage fluctuation V_1 in the time domain. Fig. 6 shows the detected voltage fluctuation V_1 and V_5 with phase stabilization. The PZT input voltage required to stabilize the fluctuation was about 130 V, and we estimated that the phase drift in our stabilization system is 6.5∼13π, because the half-wave voltage of PZT is 10∼20 V.

Fig. 7 shows the relative phase noise intensity spectra. The phase noise below the Fourier frequency of 20 Hz decreased significantly with phase stabilization. In our system, the influence introduced by the oscillator generating the dither signal is small compared to the phase noise of the optical signal.

To verify the generation of a coherent carrier, we conducted a proof-of-concept data transmission experiment based on on-off

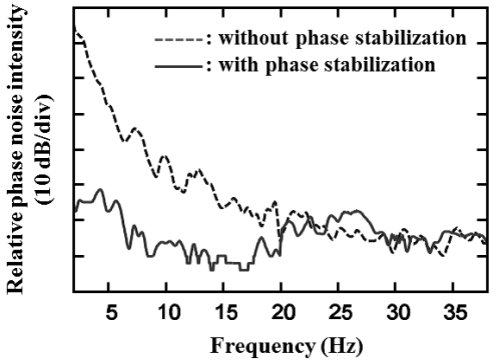

Fig. 7. Relative phase noise intensity spectra of V_1.

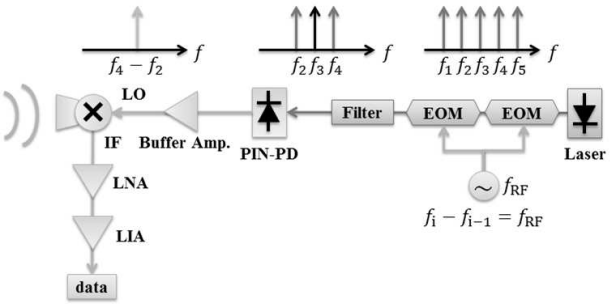

Fig. 8. Schematic diagram of the coherent receiver using subharmonic mixer.

keying modulation and heterodyne detection schemes. The carrier frequency of 100 GHz ($f_5 - f_1 = 100$ GHz) was chosen because of the availability of a uni-traveling-carrier photodiode (UTC-PD) and a detector in the transmitter and receiver, respectively. For the data signal, we used a $2^{15} - 1$ pseudo-random bit stream (PRBS) at a bit rate up to 8.5 Gbit/s. The data signal was amplified using a driver amplifier with the bandwidth of 8 GHz and the output power of 27 dBm, and applied to the MachZehnder modulator (MZM) with the bandwidth of 20 GHz for the on-off keying modulation.

On the detection side, the OFC, which is the same as the one used in the transmitter, was filtered with a wavelength filter in a single pass to generate an (local oscillator) LO signal for a sub harmonic mixer (SHM), as shown in Fig. 8. The electrical LO signal ($f_4 - f_2 = 50$ GHz) generated by photo-mixing at PIN-PD with the bandwidth of 60 GHz was amplified by an LO buffer amplifier with a bandwidth of 20 GHz (from 40 GHz to 60 GHz) and a gain of 30 dB. Note that unnecessary frequency components ($f_3 - f_2$, $f_4 - f_3 = 25$ GHz) were eliminated due to the band-limitation of the LO buffer amplifier. The LO signal was supplied to the SHM (bandwidth: 75∼110 GHz) to realize heterodyne detection. IF bandwidth of the mixer is from DC to 10 GHz and the conversion loss is about 5 dB. The SHM demodulated the 100 GHz waves and output the recovered data signals. The data signal was amplified by a low-noise amplifier (LNA) with a bandwidth of 3 kHz to 18 GHz and a gain of 30 dB, and sharpened by a limiting amplifier (LIA). An LIA covering a maximum bit-rate of 3.2 Gbit/s was used for the transmission of 3 Gbit/s, and one covering 10.6 Gbit/s was used for the transmission above 3 Gbit/s. The lower cutoff frequencies of the two LIAs are 20 kHz and 60 kHz, respectively. Therefore the fundamental component of the dither signals, 12.8 kHz and 16 kHz, can be filtered.

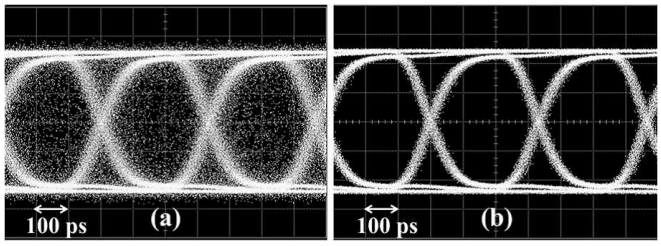

Fig. 9. Eye patterns at 3.0 Gbit/s: (a) Without phase stabilization and (b) with phase stabilization.

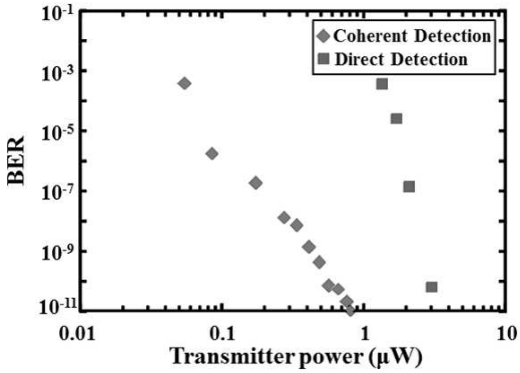

Fig. 10. BER characteristics at 1.5 Gbit/s. The PZT is used as PS in the coherent system.

IV. TRANSMISSION RESULT AND DISCUSSION

First, we tried to measure the eye patterns without phase stabilization, but were not able to obtain a stable pattern over a long time (at least 30 s), due to the uncorrelated phase fluctuations of the two optical signals used for generating the 100 GHz carrier signal.

Figs. 9(a) and 9(b) show the eye pattern at 3.0 Gbit/s without and with phase stabilization, respectively. When a PZT was used as the PS, the maximum bit rate was 5.0 Gbit/s under the error-free condition (BER $< 10^{-11}$). However, a bit rate of more than 5.0 Gbit/s under the error-free condition could not be achieved. The main reason is the jitter caused by the leak of higher harmonics of the dither signal including the frequency components higher than the low cutoff frequency of the LIA.

For comparison, we conducted a data transmission experiment with direct detection using a Schottky barrier diode as a detector. Fig. 10 shows the evaluation of the BER against the transmission power at 1.5 Gbit/s. The transmission power for the error-free condition in the heterodyne detection was 0.77 μW, whereas that for the direct detection was 3.04 μW. A sensitivity improvement of about 6 dB was obtained in the case of error-free condition.

The PZT performs phase modulation via the vibration of the piezoelectric element causing the harmonics, while the EOM

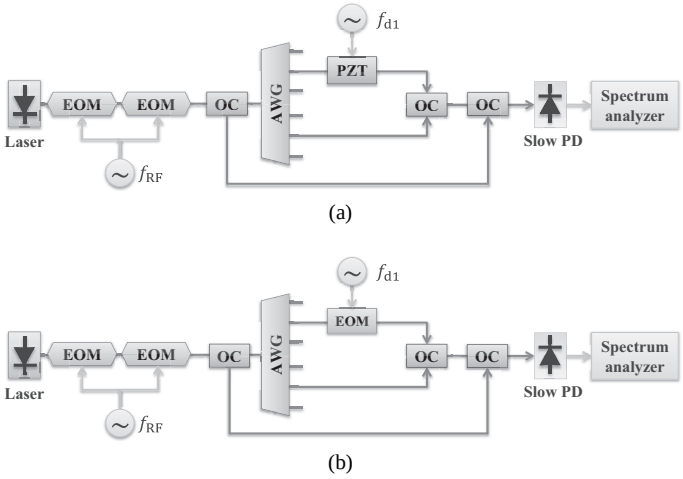

Fig. 11. Schematic diagram of observing harmonic intensity with: (a) PZT and (b) EOM.

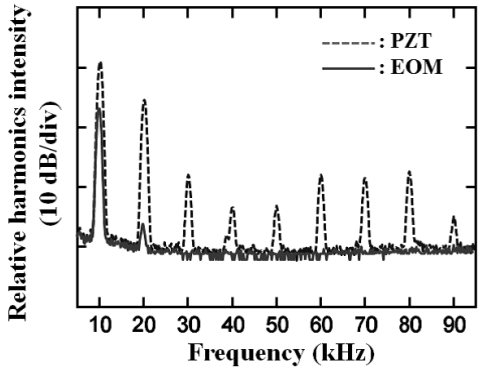

Fig. 12. Relative harmonics intensity spectra.

performs it by using a change in the refractive index of the material, e.g., $LiNbO_3$. Thus, harmonics is less likely to occur when using the EOM than when using the PZT. We confirmed the difference in harmonics between using the PZT and using the EOM with the bandwidth of 20 GHz with experimental systems, as shown in Figs. 11(a) and 11(b). The dither signal is applied to one frequency component of the optical carriers extracted from the AWG filter with PZT or with EOM. By using a PD with a cutoff frequency below f_{RF}, higher harmonic components are output.

Fig. 12 shows the relative harmonics intensity spectra. The dither frequency was 10 kHz and the cutoff frequency of the PD was 320 kHz. When using PZT, the output of the PD included the ninth harmonic at least. On the other hand, when using EOM, the output included the second harmonic at least. In this experiment, we did not observe a leak of harmonics higher than the low cutoff frequency of the LIA by using EOM.

The half-wave voltage of the EOM is 4.5 V, and the locking range is only up to 3.1π due to the limited maximum input voltage of 14 V. The phase drift in our system is approximately $6.5\sim13\pi$. Therefore, the phase fluctuations are not compensated for a long time required to measure BER in a data transmission when the EOM is used for both dither and feedback. On

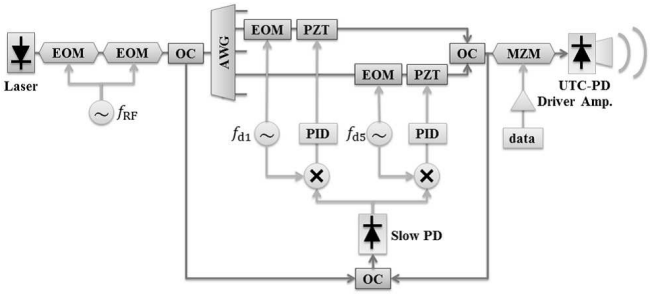

Fig. 13. Schematic diagram of the coherent sub-THz wave generator with a novel phase stabilization system.

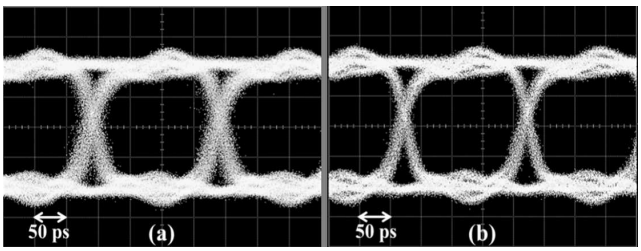

Fig. 14. Eye pattern at 5.0 Gbit/s using: (a) PZT and (b) PZT and EOM.

the other hand, the half-wave voltage of PZT is 10∼20 V, and the limited maximum input voltage is 150 V. Thus, the locking range of the PZT is up to $7.5\sim15\pi$, and the phase fluctuation is stabilized when the PZT is used for control.

On the other hand, our novel phase stabilization system uses both EOM and PZT. Fig. 13 shows a schematic diagram of the coherent sub-THz wave generator with our system. In this system, EOMs are used to apply dither signals to optical frequency components. The phase fluctuations detected as voltage fluctuations by two-stage down-conversion are negatively fed back to the PZTs with PID controllers. By using this system, higher harmonics are less likely to occur, and the phases of the optical carrier signals are stabilized more effectively than with the previous system.

Figs. 14(a) and 14(b) show the eye pattern at 5.0 Gbit/s with the phase stabilization using the PZT, and with the novel phase stabilization using the PZT and the EOM, respectively. In the case of our phase stabilization method, the spread of the jitter caused by the leak of higher harmonics from the PZT does not occur, and the maximum bit rate of 8.5 Gbit/s under the error-free condition is successfully achieved, as shown in Fig. 15.

The main reason we have not achieved a bit rate of more than 8.5 Gbit/s under the error-free condition is the band-limitation of the amplifier used to drive the data signal. If the amplifier is changed to one with a wide bandwidth, e.g., 20 GHz, we can expect to achieve a bit rate of more than 10 Gbit/s.

It is also necessary to consider how the phase noise of the oscillator generating the OFC affects the phases of the sub-THz carrier signal and the BER performance. Theoretically, the phase noise of the carrier signal generated from an OFC signal is increased by $20\log(x)$ compared to that of the oscillator, where x is the multiplication order [16]. For $f_{\mathrm{RF}} = 25\,\mathrm{GHz}$, the phase noise of the oscillator is approximately $-100\,\mathrm{dBc/Hz}$ at the off-

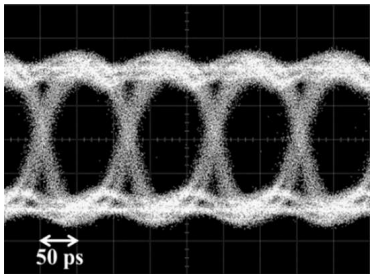

Fig. 15. Eye pattern at 8.5 Gbit/s with the novel phase stabilization.

set frequency of 10 kHz. Therefore, for the carrier frequency of 100 GHz ($f_5 - f_1 = 100\ \mathrm{GHz}$), the estimated phase noise at the offset frequency of 10 kHz is $-88\ \mathrm{dBc/Hz}$. In theory, the phase noise causes the BER floor. In our experiment, since no floor was observed, we can conclude that the phase noise was not so large as to degrade the BER performance.

Our coherent carrier generation scheme can be applied to higher frequencies, e.g., 300 GHz and is immediately amenable to the multi-carrier modulation of OFDM.

V. CONCLUSION

We have described a photonics-based approach to generating phase-locked sub-THz carrier signals with a new stabilization method, and have successfully demonstrated a data transmission up to 8.5 Gbit/s based on on-off keying modulation and heterodyne detection schemes at 100 GHz carrier frequency. Future work will have to address the issue of increasing in the carrier frequency to 300 GHz or more for achieving a data rate of over 40 Gbit/s. Also, we should work towards perfecting an approach that is applicable to multi-level modulation formats towards 100 Gbit/s.

ACKNOWLEDGMENT

The authors would like to thank Prof. K. Iwatsuki from Tohoku University and Mr. T. Mukumoto for their support throughout this research. This work was supported in part by the JST-ANR WITH program.

REFERENCES

[1] T. Nagatsuma, H. -J. Song, and Y. Kado, "Challenges for ultrahigh speed wireless communications using Terahertz waves," *J. Terahertz Sci. Technol.*, vol. 3, no. 2, pp. 55–65, 2010.

[2] T. Nagatsuma, T. Takada, H. -J. Song, K. Ajito, N. Kukutsu, and Y. Kado, "Millimater- and THz-wave photonics towards 100 Gbit/s wireless transmission," in *Proc. Meeting IEEE Photon. Soc.*, 2010, pp. 385–386.

[3] H. -J. Song, K. Ajito, Y. Muramoto, A. Wakatsuki, T. Nagatsuma, and N. Kukutsu, "24 Gbit/s data transmission in 300 GHz band for future Terahertz communications," *Electron. Lett.*, vol. 48, no. 15, pp. 953–954, 2012.

[4] T. Nagatsuma, "Generating millimeter and Terahertz waves by photonics for communications and sensing," *Tech. Dig. IMS*, WE2H-1, 2013.

[5] X. Pang, A. Caballero, A. Dogadaev, V. Arlunno, L. Deng, R. Borkowski, J. S. Pedersen, D. Zibar, X. Yu, and I. T. Monroy "25 Gbit/s QPSK hybrid fiber-wireless transmission in the W-band (75–110 GHz) with remote antenna unit for in-building wireless networks," *IEEE Photon. J.*, vol. 4, no. 3, pp. 691–698, 2012.

[6] L. Deng, M. Beltran, X. Pang, X. Zhang, V. Arlunno, Y. Zhao, A. Dogadaev, X. Yu, R. Llorente, D. Liu, and I. T. Monroy, "Fiber-wireless transmission of 8.3 Gb/s/ch QPSK-OFDM signals in 75–100 GHz band" *Opt. Lett.*, vol. 37, no. 24, pp. 5106–5108, 2012.

[7] D. Zibar, R. Sambaraju, A. C. Jambrina, J. Herrera, and I. T. Monroy, "Carrier recovery and equalization for photonic-wireless links with capacities up to 40 Gb/s in 75–110 GHz Band," in *Proc. Opt. Fiber Conf.*, 2011, pp. 1–3.

[8] X. Pang, A. Caballero, A. Dogadaev, V. Arlunno, R. Borkowski, J. S. Pedersen, L. Deng, F. Karinou, F. Roubeau, D. Zibar, X. Yu, and I. Tafur Monroy, "100 Gb/s hybrid optical fiber-wireless link in the W-band (75–110 GHz)," *Opt. Exp.*, vol. 19, no. 25, pp. 24944–24949, 2011.

[9] M. Beltrn, L. Deng, X. Pang, X. Zhang, Y. Zhao, X. Yu, R. Llorente, D. Liu, I. T. Monroy, "Single- and multiband OFDM photonic wireless links in the 75-110 GHz band employing optical combs," *IEEE Photon. J.*, vol. 4, no. 5, pp. 2027–2036, 2012.

[10] L. Deng, D. M. Liu, X. D. Pang, X. Zhang, V. Arlunno, Y. Zhao, A. Caballero, A. K. Dogadaev, X. B. Yu, I. T. Monroy, M. Beltran, and R. Llorente, "42.13 Gbit/s 16QAM-OFDM photonics-wireless transmission in 75–110 GHz band," *Progress Electromagn. Research*, vol. 126, pp. 449–461, 2012.

[11] A. Kanno, K. Inagaki, I. Morohashi, T. Sakamoto, T. Kuri, I. Hosako, T. Kawanishi, Y. Yoshida, and K. Kitayama, "20-Gb/s QPSK W-band (75–110 GHz) wireless link in free space using radio-over-fiber technique," *IEICE Electron. Exp.*, vol. 8, no. 8, pp. 612–617, 2011.

[12] A. Kanno, K. Inagaki, I. Morohashi, T. Sakamoto, T. Kuri, I. Hosako, T. Kawanishi, Y. Yoshida, and K. Kitayama, "40 Gb/s W-band (75–110 GHz) 16-QAM radio-over-fiber signal generation and its wireless transmission," *Opt. Exp.*, vol. 19, no. 26, pp. B56–B63, 2011.

[13] A. Hirata, H. Togo, N. Shimizu, H. Takahashi, K. Okamoto, and T. Nagatsuma, "Low-phase noise photonic millimeter-wave generator using an AWG integrated with a 3-dB combiner," *IEICE Trans. Electron.*, vol. E88-C, no. 7, pp. 1458–1464, 2005.

[14] L. Moller, J. Federici, A. Sinyukov, C. Xie, H. C. Lim, and R. C. Giles, "Data encoding on Terahertz signals for communication and sensing," *Opt. Lett.*, vol. 33 no. 4, pp. 393–395, 2008.

[15] K.-H. Ang, G. Chong, and Y. Li, "PID control system analysis, design, and technology," *IEEE Trans. Control Syst.*, vol. 13, no. 4, 2005.

[16] H.-J. Song, N. Shimizu, T. Furuta, K. Suizu, H. Ito, T. Nagatsuma, H. Song, and S. member, "Broadband-frequency-tunable sub-terahertz wave generation using an optical comb, AWGs, optical switches, a uni-traveling carrier photodiode for spectroscopic applications," *J. Lightw. Technol.*, vol. 26, no. 15, pp. 2521–2530, 2008.

Yasuyuki Yoshimizu was born in Ishikawa, Japan, on November 2, 1989. He received his B.S. degree in Engineering Science from Osaka University, Osaka, Japan in 2013. In 2013, he entered the Graduate School of Engineering Science, Osaka University. His current research includes THz wireless communication system.

Shintaro Hisatake was born in Kochi, Japan, on April 12, 1976. He received the M.E. and Ph.D. degrees in Electronic Engineering from Doshisha University, Kyoto, Japan in 2000 and 2003, respectively. He was engaged in the development of frequency stabilization and linewidth reduction techniques for visible laser diodes from 2000 to 2003. In 2003, he joined the Graduate School of Engineering Science, Osaka University, Osaka, Japan, where he is currently an Assistant Professor and involved optical signal processing based on high-frequency electronics and THz wave generation, modulation, and detection based on photonics. Dr. Hisatake is a Member of the OSA, IEICE, and JSAP.

Shigeru Kuwano received the B.E., M.E., and Ph.D. degrees in Communication Engineering, from Osaka University, Osaka, Japan in 1987, 1989, and 1992, respectively. He joined NTT Corporation in 1992, where he engaged in research and development of the optical transmission system, optical networking, LAN technology based networks, and wireless system. He is now a Senior Research Engineer of NTT Access Network Service Systems Laboratories, and working on the research and development of optical and wireless converged networks. He is a Member of the Institute of Electrical and Electronics Engineers (IEEE) and the Institute of Electronics, Information and Communication Engineers (IEICE) of Japan.

Jun Terada received the B.E. and M.E. degrees from Keio University, Kanagawa, Japan in 1993 and 1995, respectively. In 1995, he joined the NTT LSI Laboratories, where he was engaged in research on low-voltage analog circuits and high-speed front-end circuits for optical transceivers. He is now a Senior Research Engineer and a Supervisor at the NTT Access Network Service Systems Laboratories, where he is responsible for R&D management of optical and wireless converged access networks. He has served on the Technical Program Committees of the Symposium on VLSI Circuits and Asian Solid-State Circuits Conference (A-SSCC). He is a Member of the Institute of Electrical and Electronics Engineers (IEEE) and the Institute of Electronics, Information and Communication Engineers (IEICE) of Japan.

Naoto Yoshimoto received B.S., M.S., and Ph.D. degrees in Electronics and Information Engineering from Hokkaido University, Japan in 1986, 1988, and 2003, respectively. He joined NTT Laboratories in 1988, and engaged in the research and development of optical transmission equipment and related optical modules for broadband access systems. He is currently the Project Manager of Optical Access System Project in NTT Access Network Service Systems Laboratories, and is engaged in the planning and design of next-generation optical access networks and architectures mainly based on high-speed TDM-PON and future advanced PON technologies. He is a Member of the IEEE Communication Society and a Senior Member of the Institute of Electronics, Information and Communication Engineers (IEICE) of Japan.

Tadao Nagatsuma received B.S., M.S., and Ph.D. degrees in Electronic Engineering from Kyushu University, Fukuoka, Japan in 1981, 1983, and 1986, respectively. From 1986 to 2007, he was with Nippon Telegraph and Telephone Corporation (NTT), Atsugi, Kanagawa, Japan. Since 2007, he has been a Professor at Graduate School of Engineering Science, Osaka University. His research interests include millimeter-wave and terahertz photonics and their application to sensors and wireless communications. Prof. Nagatsuma is a Fellow of the Institute of Electronics, Information and Communication Engineers (IEICE), Japan, a Senior Member of the IEEE, and Members of the Technical Committee on Microwave Photonics of the IEEE Microwave Theory and Techniques Society, and the Microwave Photonics Steering Committee, and serves as an Associate Editor of the IEEE Photonics Technology Letters. He is the recipient of numerous awards including the 1992 IEEE Andrew R. Chi Best Paper Award, the 1997 Okochi Memorial Award, the 1998 Japan Microwave Prize, the 2000 Ministerfs Award of the Science and Technology Agency, the 2002 Asia-Pacific Microwave Conference Prize, the 2004 Yokosuka Research Park Award, the 2006 Asia-Pacific Microwave-Photonics Conference Award, the 2006 European Microwave Conference Prize, the 2007 Achievement Award presented by the IEICE, the 2008 Maejima Award presented by the Post and Telecom Association of Japan, the 2011 Commendation for Science and Technology by the Minister of Education, Culture, Sports, Science and Technology, the 2011 Recognition from Kinki Bureau of Telecommunications, Ministry of Internal Affairs and Communications, the 2011 Asia-Pacific Microwave Conference Prize, the 2012 Osaka University Presidential Awards for Achievement, and the 2013 Nikkei Electronics Japan Wireless Technology Award.